PCP
PLANT & CELL PHYSIOLOGY

Metabolic consequences of knocking out *UGT85B1*, the gene encoding the glucosyltransferase required for synthesis of dhurrin in *Sorghum bicolor* (L. Moench)

Cecilia K. Blomstedt[1], Natalie H. O'Donnell[1,4], Nanna Bjarnholt[2], Alan D. Neale[1], John D. Hamill[1,5], Birger Lindberg Møller[2,3] and Roslyn M. Gleadow[1,*]

[1]School of Biological Sciences, Monash University, Wellington Rd, Clayton, 3800 Australia
[2]Plant Biochemistry Laboratory and VILLUM research center for 'Plant Plasticity', Department of Plant and Environmental Sciences, University of Copenhagen, 40 Thorvaldsensvej, DK-1871 Frederiksberg C, Copenhagen, Denmark
[3]Carlsberg Laboratory, Gamle Carlsberg Vej 10, DK-1799 Copenhagen V, Denmark
[4]Present address: Plant Health Australia, level 1, 1 Phipps Close, Deakin, 2600 Australia.
[5]Present address: Centre for Regional and Rural Futures (CeRRF), Deakin University, 75 Pigdons Rd, Waurn Ponds, 3216, Australia.
*Corresponding author: E-mail, ros.gleadow@monash.edu; Fax, +61-3-9905-5613.
(Received June 26, 2015; Accepted October 12, 2015)

Many important food crops produce cyanogenic glucosides as natural defense compounds to protect against herbivory or pathogen attack. It has also been suggested that these nitrogen-based secondary metabolites act as storage reserves of nitrogen. In sorghum, three key genes, *CYP79A1*, *CYP71E1* and *UGT85B1*, encode two Cytochrome P450s and a glycosyltransferase, respectively, the enzymes essential for synthesis of the cyanogenic glucoside dhurrin. Here, we report the use of targeted induced local lesions in genomes (TILLING) to identify a line with a mutation resulting in a premature stop codon in the N-terminal region of *UGT85B1*. Plants homozygous for this mutation do not produce dhurrin and are designated *tcd2* (*totally cyanide deficient* 2) mutants. They have reduced vigor, being dwarfed, with poor root development and low fertility. Analysis using liquid chromatography–mass spectrometry (LC-MS) shows that *tcd2* mutants accumulate numerous dhurrin pathway-derived metabolites, some of which are similar to those observed in transgenic Arabidopsis expressing the *CYP79A1* and *CYP71E1* genes. Our results demonstrate that *UGT85B1* is essential for formation of dhurrin in sorghum with no co-expressed endogenous UDP-glucosyltransferases able to replace it. The *tcd2* mutant suffers from self-intoxication because sorghum does not have a feedback mechanism to inhibit the initial steps of dhurrin biosynthesis when the glucosyltransferase activity required to complete the synthesis of dhurrin is lacking. The LC-MS analyses also revealed the presence of metabolites in the *tcd2* mutant which have been suggested to be derived from dhurrin via endogenous pathways for nitrogen recovery, thus indicating which enzymes may be involved in such pathways.

Keywords: Cyanogenic glucoside • Detoxification • Dhurrin • Metabolic turnover • Sorghum • UDP-glycosyltransferase.

Abbreviations: CN^--N/N%, allocation of nitrogen to dhurrin; EMS, ethyl methanesulfonate; ER, endoplasmic reticulum; F_v/F_m, variable fluorescence/maximal fluorescence; HCNp, hydrogen cyanide potential; LC-MS, liquid chromatography–mass spectrometry; NO_3^--N/N%, allocation of nitrogen to nitrate; *tcd2*, totally cyanide deficient mutant; *TCD2*, sibling line to the mutant; TILLING, targeted induced local lesions in genomes; UGT, UDP-glycosyltransferase.

Introduction

Cyanogenic glucosides are classified as phytoanticipins, and are widespread throughout the plant kingdom, constituting a defense against herbivores and pests (Møller 2010a, Møller 2010b, Gleadow and Møller 2014). The detailed study of cyanogenic glucoside biosynthesis was first undertaken in *Sorghum bicolor* (L. Moench), and the basic biochemical pathway has since been shown to be very similar across many plant species (reviewed in Gleadow and Møller 2014). In sorghum, the cyanogenic glucoside dhurrin is derived from the amino acid L-tyrosine by the sequential action of two Cyt P450s, CYP79A1 and CYP71E1, to produce an α-hydroxynitrile (Sibbesen et al. 1995, Kahn et al. 1997, Bak et al. 1998), which is then glucosylated by a UDP-glucose:*p*-hydroxymandelonitrile-*O*-glucosyltransferase UGT85B1 (Jones et al. 1999, Hansen et al. 2003) (**Fig. 1**). The glucosylation stabilizes the labile cyanohydrin. The Cyt P450s form part of a metabolon that is anchored within the endoplasmic reticulum (ER), and the pathway is highly channeled through the metabolon to prevent accumulation of reactive and toxic intermediates that are formed during synthesis (Møller and Conn 1980, Jørgensen et al. 2005, Nielsen et al. 2008, Jensen et al. 2011, Laursen et al. 2015). CYP79A1 catalyzes the first step in dhurrin synthesis, the conversion of L-tyrosine into *p*-hydroxyphenylacetaldoxime (Sibbesen et al. 1995), which is rate limiting and shows high substrate specificity (Kahn et al. 1999, Busk and Møller 2002). In contrast, in vitro studies suggest that UGT85B1 possesses broader substrate specificity, but it has been proposed that in planta substrate specificity is high (Kristensen et al. 2005, Morant et al. 2007).

Plant Cell Physiol. 57(2): 373–386 (2016) doi:10.1093/pcp/pcv153, Advance Access publication on 22 October 2015, available online at www.pcp.oxfordjournals.org

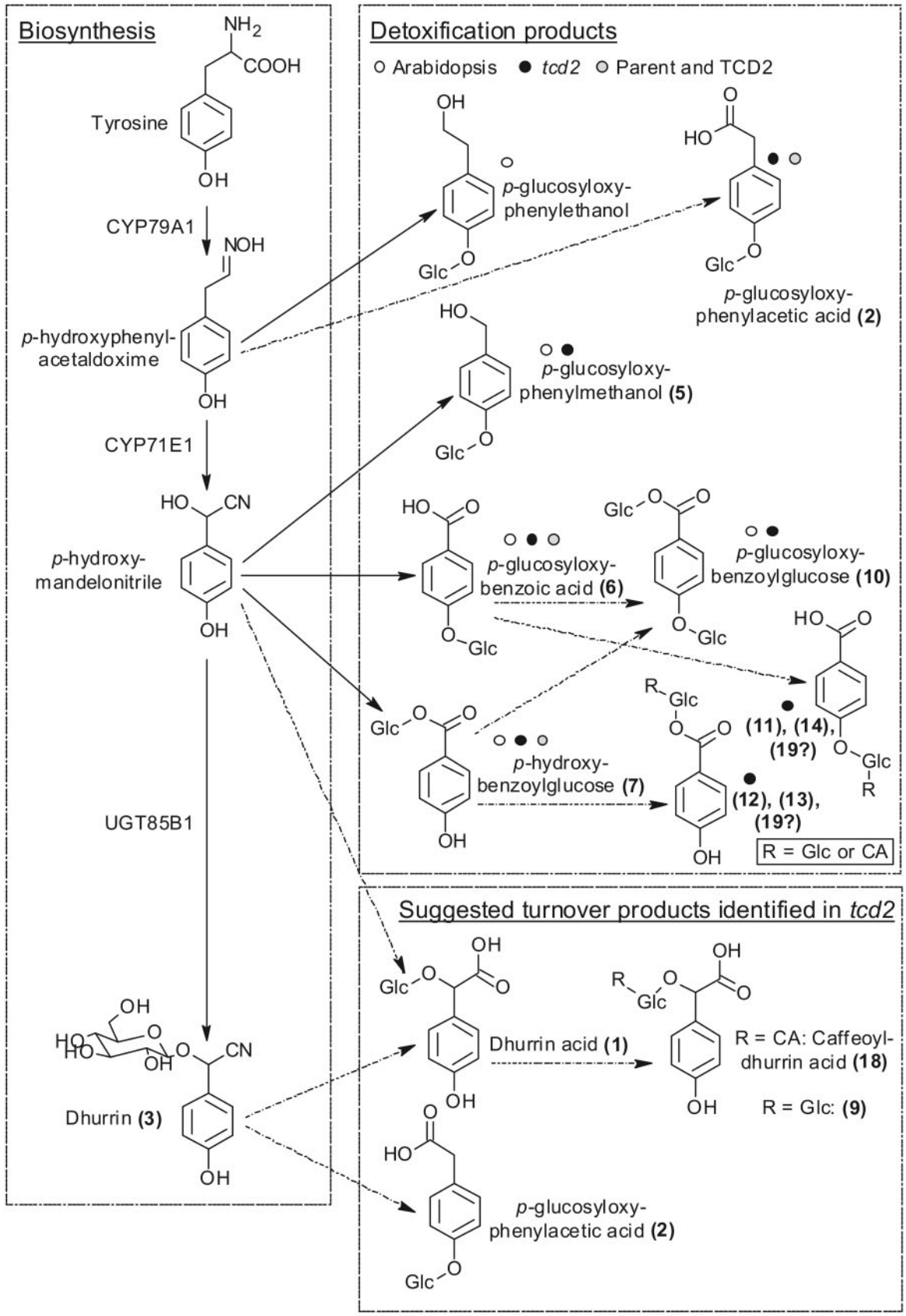

Fig. 1 Dhurrin biosynthesis in sorghum and the formation of products derived from the different intermediates as part of the detoxification processes or as putative turnover products identified in the *tcd2* mutant in the present study. Solid arrows signify previously assigned reactions and products. Dashed arrows are putative reactions proposed based on the current study. Structure numbers refer to **Fig. 6** and **Table 1**. Listed compounds were previously identified in Kristensen et al. (2005) (Arabidopsis 2x) or in Pičmanová et al. (2015) (sorghum).

Genes from the sorghum pathway for biosynthesis of dhurrin have been transferred to other species, including *Arabidopsis thaliana*, *Nicotiana tabacum* (tobacco), *Vitis vinifera* (grapevine) and *Lotus japonicus* (Lotus) (Bak et al. 2000, Tattersall et al. 2001, Kristensen et al. 2005, Franks et al. 2006). When all three biosynthetic genes, *CYP79A1*, *CYP71E1* and *UGT85B1*, were inserted into normally acyanogenic Arabidopsis, transgenic plants accumulated up to 4% dry weight dhurrin with only minor effects on plant morphology (Bak et al. 1999, Tattersall et al. 2001, Kristensen et al. 2005). Dhurrin accumulation in these transgenic Arabidopsis plants also conferred resistance to flea beetles (Tattersall et al. 2001). However, when genes encoding the two Cyt P450s, but not *UGT85B1*, were transformed into Arabidopsis, transgenic plants (designated Arabidopsis 2x) were stunted and grew poorly. These transgenic plants did not accumulate dhurrin, but liquid chromatography–mass spectrometry (LC-MS) analysis showed the presence of several novel metabolites, which were probably detoxification products of the oxime and cyanohydrin (*p*-hydroxymandelonitrile) intermediates of the dhurrin pathway (Kristensen et al. 2005) (**Fig. 1**). These studies indicated that the sequential action of CYP79A1, CYP71E1 and UGT85B1 enables dhurrin synthesis in Arabidopsis without accumulation of intermediates or by-products that are deleterious to growth (Kristensen et al. 2005). Similar results were observed for transformation of the genes encoding dhurrin biosynthesis into tobacco, grapevine or Lotus, indicating that none of the co-expressed endogenous UDP-dependent glycosyltransferases (UGTs) was capable of glycosylating the cyanohydrin, hydroxymandelonitrile (Franks et al. 2006, Morant et al. 2007).

Plant family 1 UGTs catalyze glycosylation of a plethora of bioactive natural products (Osmani et al. 2009). They constitute a highly divergent, multienzyme family (Paquette et al. 2003, Bowles and Lim 2010). Glycosylation serves to stabilize and thereby secure safe storage of a wide range of primary and secondary metabolites. Plant family 1 glucosyltransferases are characterized by a 44 amino acid sequence in the C-terminal domain of the protein, termed the putative secondary plant glycosyltransferase (PSPG) motif, which is involved in binding the sugar donor (Paquette et al. 2003, Osmani et al. 2009, Bowles and Lim 2010). Outside this region there is little sequence similarity across UGTs, and substrate specificity cannot be predicted from sequence alignments. Homology modeling of UGT85B1 against determined crystal structures from characterized UGTs has indicated that a specific 33 amino acid sequence, termed Loop B, may have a role in associating the UGT with the P450s and is important in facilitating metabolon formation (Thorsøe et al. 2005, Osmani et al. 2009). Alignment of the Loop B sequence of sorghum UGT85B1 with the equivalent region in UGTs from two other cyanogenic species, cassava (*Manihot esculenta*; UGT85K4 and UGT85K5; Kannangara et al. 2011) and almond (*Prunus dulcis*; UGT85A19; Franks et al. 2008), results in relatively high sequence similarity (75–80%), supporting the hypothesized role in the metabolon.

Use of targeted induced local lesions in genomes (TILLING; Till et al. 2003) has enabled mutations in the genes encoding the first Cyt P450 of the pathway to be identified in *L. japonicus* (Takos et al. 2010) and *Sorghum bicolor* (Blomstedt et al. 2012). A number of sorghum lines possessing mutations in the coding region of the *UGT85B1* gene were also obtained (Blomstedt et al. 2012). In the current report we demonstrate that sorghum plants homozygous for a mutation resulting in a premature stop codon in the coding sequence of *UGT85B1* are totally deficient in dhurrin synthesis. In concordance with our earlier study (Blomstedt et al. 2012), we designate this mutant as *tcd2* (totally cyanide deficient mutant line type 2).

Results

Identification of the mutation in *tcd2*

TILLING analysis identified several sorghum lines with mutations in the gene encoding the family 1 glucosyltransferase UGT85B1 (Blomstedt et al. 2012). Sequencing of the *UGT85B1* gene from the *tcd2* line identified a mutation resulting in a C to T change that generates a stop codon at Q149* in the deduced protein sequence (**Supplementary Fig. S1**). No difference was seen in the nucleotide (data not shown) or the deduced protein sequence of *TCD2*-sibling lines compared with the parental control line (**Supplementary Fig. S1**). A protein BLAST search of the sorghum genome (http://phytozome.jgi.doe.gov/pz/portal.html#!search) using the full-length UGT85B1 coding sequence identified >200 UGTs present in sorghum, based mainly on identity within the PSPG motif. In contrast, when the Loop B sequence was used in the protein Blast search only four UGTs were identified. Protein sequence alignment of UGT85B1 with the four additional UGTs, as well as UGTs from the cyanogenic species, cassava and Lotus, showed 45–50% identity overall (**Supplementary Fig. S2**; **Supplementary Table S1A**), with variable homology in the Loop B region, ranging from 35% to 67% (**Supplementary Fig. S2**; **Supplementary Table S1B**). It is noteworthy that none of the additional four UGTs from sorghum is located on chromosome 1, where the *CYP79A1*, *CYP71E1* and *UGT85B1* genes required for dhurrin synthesis are clustered. Gene clustering is thought to promote co-regulation of expression and metabolon formation (Takos et al. 2011).

Growth characteristics of the *tcd2* mutant sorghum line

Analysis of growth parameters showed that *tcd2* plants homozygous for the *UGT85B1* mutation had reduced stature and vigor compared with *TCD2* sibling and parental control lines (**Fig. 2A, B**; **Supplementary Table S2**). When harvested 8 weeks post-germination, *tcd2* plants were significantly shorter compared with the parental control and *TCD2* sibling lines ($P < 0.001$). Mutant *tcd2* plants also exhibited a significant decrease ($P < 0.05$) in leaf surface area, leaf length and width compared with parental controls and *TCD2* siblings (**Fig. 2C**; **Supplementary Table S2**). No statistically significant difference in total shoot or root mass between lines was found in plants harvested 8 weeks post-germination (**Fig. 2B**). In plants

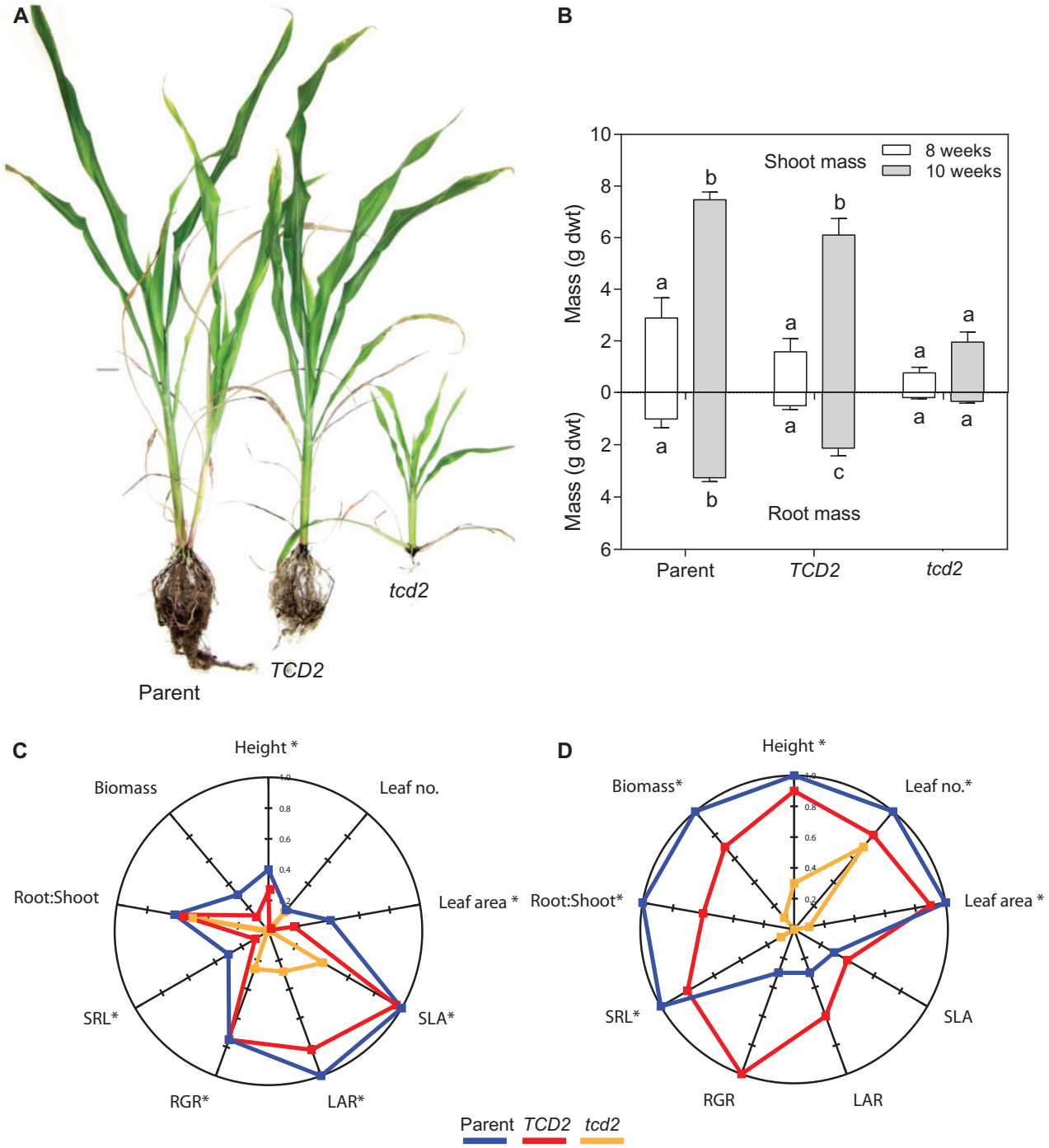

Maximum values: Biomass (total) 10.7g; Height 144 mm; Leaf number 12; Leaf area 918 cm^2; Specific Leaf Area (SLA) 9734 cm g^{-1}; Leaf Area Ratio (LAR) 66.8 m^2 g^{-1}; Relative Growth Rate (RGR) 90 mg g^{-1}; Specific Root Length (SRL) 9.73 m g^{-1}; Root:Shoot ratio 0.44.

Fig. 2 (A) Phenotype of parental control, *TCD2* sibling control and *tcd2* sorghum plants recorded 10 weeks after germination; (B) mean mass ± 1 SE (g dwt) of shoots and roots measured 8 and 10 weeks after germination, respectively. (C) Rose plots of key biometric data obtained 8 and 10 weeks post-germination. For each parameter, values were normalized against the largest numerical value (shown in parentheses) obtained for either parental, *TCD2* or *tcd2* plants. Means that were significantly different are indicated with an asterisk (see **Supplementary Table S1** for a full statistical analysis). The parental control line is the line used in the initial EMS study (Blomstedt et al. 2012), the *tcd2* line is acyanogenic and has a mutation in *UGT85B1*, and *TCD2* is the cyanogenic sibling to *tcd2*, selected for wild-type *UGT85B1*.

harvested 10 weeks post-germination, the *tcd2* plants were significantly smaller than parental controls (**Fig. 2A, D**). The *TCD2* siblings were intermediate in size between the *tcd2* plants and the parental controls, with significant differences among lines in all parameters measured, except stem width and the width of leaf III (**Fig. 2**; **Supplementary Table S2**).

Several additional parameters were used to evaluate the growth rate and biomass partitioning, and these indicated that the *tcd2* line was negatively affected by the mutation in UGT85B1. The major difference was seen in specific root length (SRL) where *tcd2* roots were significantly shorter than parental controls at both harvest times (**Fig. 2C, D**; **Supplementary Table S3**). The root : shoot ratio of *tcd2* plants was also significantly lower than that of both the parental controls and the *TCD2* sibling line in plants harvested 10 weeks post-germination (**Fig. 2D**; **Supplementary Table S3**). In plants harvested 8 weeks post-germination, the relative growth rate (RGR), the specific leaf area (SLA) and the leaf area ratio (LAR) of the *tcd2* plants were significantly reduced compared with the parental control plants. These differences were not observed in plants harvested 10 weeks post-germination (**Fig. 2D**; **Supplementary Table S3**). The net assimilation rate (NAR) and leaf weight ratio (LWR) did not differ between *tcd2* and the parent control line at the two harvest points (**Supplementary Table S3**). The overall differences in plant growth of various lines are illustrated in the rose plots, where the *tcd2* plants exhibit a much reduced plot area (**Fig. 2C, D**).

To determine whether the *tcd2* mutant was affected in photosynthetic capacity, an analysis of the pigment levels and PSII efficiency was conducted. At both harvest points, no significant differences were observed between *tcd2* and parental or *TCD2* control lines with respect to carotenoid concentrations, Chl *a*/*b* ratios or Chl*a* + Chl*b* concentrations (**Supplementary Table S4**). The efficiency of PSII, measured by F_v/F_m, also did not vary for leaf I or leaf III of either harvest time point for the *tcd2* plants. However, the F_v/F_m of leaf III in both parental and *TCD2* control lines harvested 10 weeks post-germination was reduced compared with the *tcd2* plants, although this reduction was only significant in the *tcd2* and parental control line comparison ($P < 0.01$; **Supplementary Fig. S3**). Reproductive potential was also impaired in *tcd2* mutants compared with the *TCD2* siblings. Seed set was lower and, while seeds were viable, the germination rate was also lower (data not shown).

Dhurrin, nitrate and nitrogen determination

The dhurrin concentration of the leaf blade, leaf sheath and roots was measured as the amount of hydrogen cyanide (HCN) produced following complete β-glucosidase-mediated hydrolysis of the dhurrin, also referred to as the HCN potential (HCNp). The HCNp detected in leaf, sheath and root tissues of *tcd2* plants was not significantly different from background ($<0.01\ mg\ g^{-1}$), showing that plants homozygous for the Q149* mutation lack the capacity to accumulate dhurrin (**Fig. 3A**). In contrast, the HCNp in the leaf blade and leaf sheath of the parental and *TCD2* control plants was 0.5–$1.3\ mg\ g^{-1}$ dry mass in plants harvested 8 weeks post-germination, decreasing to lower levels (0.01–$0.04\ mg\ g^{-1}$ dwt) in plants harvested 10 weeks post-germination (**Fig. 3A**). Interestingly, in the roots of parental and *TCD2* control plants, the HCNp did not decrease between the two harvest time points to the same degree as observed in the leaves and sheath. The total amount of dhurrin represented by equivalents of HCN in the shoots and roots was calculated at each harvest time by multiplying HCNp by the dry mass of each organ (**Fig. 4A**). There was no significant difference in the total amount of dhurrin in the parent and *TCD2* plants. The total content of dhurrin in the shoot of the parent and *TCD2* plants decreased strongly from 8- to 10-week-old plants, whereas the total dhurrin content of the roots was not significantly different for either line (**Fig. 4A**).

The nitrate concentration in plants harvested 8 weeks post-germination showed no significant difference in any of the tissue types and plant lines investigated (**Fig. 3B**). However, in plants harvested 10 weeks post-germination, nitrate levels in the leaf blade of the parental and *TCD2* controls were reduced whilst nitrate levels in the *tcd2* mutant remained at levels observed in the 8-week-old plants. This difference in nitrate levels was even more pronounced in the leaf sheath, resulting in a significant difference between the parental and *TCD2* controls and the *tcd2* mutant plants (**Fig. 3B**). A marked reduction in nitrate concentration in roots of parental and *TCD2* controls between harvest time points was also observed, but not in the roots of *tcd2* plants. Calculation of the total nitrate content of the shoots and roots of the plants showed that the shoots contained at least 4-fold more nitrate than the roots for all plants (**Fig. 4B**). In plants harvested 8 weeks post-germination, the total nitrate content of the *tcd2* shoots was significantly less (70%) than in the shoots of the parental control ($P = 0.013$) whereas the total nitrate content of the *TCD2* shoots was not significantly different from that of the parental control or the *tcd2* plants (**Fig. 4B**). The total nitrate content of the shoots of *tcd2* plants increased with time so that in plants harvested 10 weeks post-germination there was no significant difference in the total nitrate content in the shoots of the three lines. The total amount of nitrate in the roots of the *tcd2* plants in plants harvested 8 weeks post-germination was 75% less than in the parental control plants (**Fig. 4B**). In plants harvested 10 weeks post-germination, the parental control plants had double the total root nitrate content compared with the content in plants harvested 8 weeks post-germination. Yet the total root nitrate content of the *tcd2* and *TCD2* plants was approximately 80% lower than that of the parent plants and the nitrate concentration of the *tcd2* roots did not change between the harvest time points (**Fig. 4B**).

In terms of total nitrogen content, no significant difference was found for elemental nitrogen in the leaf blade, leaf sheath and roots of the *tcd2* mutant and the parental and *TCD2* control plants in 8-week-old plants (**Fig. 3C**). At 10 weeks post-germination, the *tcd2* plants had higher levels of elemental nitrogen in all tissue compared with the parental and *TCD2* sibling control lines, although the difference was only statistically significant ($P < 0.05$) between the mutant and control lines for leaf sheath and roots (**Fig. 3C**). When the total nitrogen content of the shoot and root tissue was calculated per plant for the two harvest time points, the shoot nitrogen content of *tcd2* plants was 70% and 60% less than in the parent, respectively (**Fig. 4C**). Interestingly, the total nitrogen content of the *TCD2* shoots was not significantly different from that of the parental control or the *tcd2* plants at either harvest time (**Fig. 4C**). The total amounts of nitrogen in the root of the parent, *TCD2* and

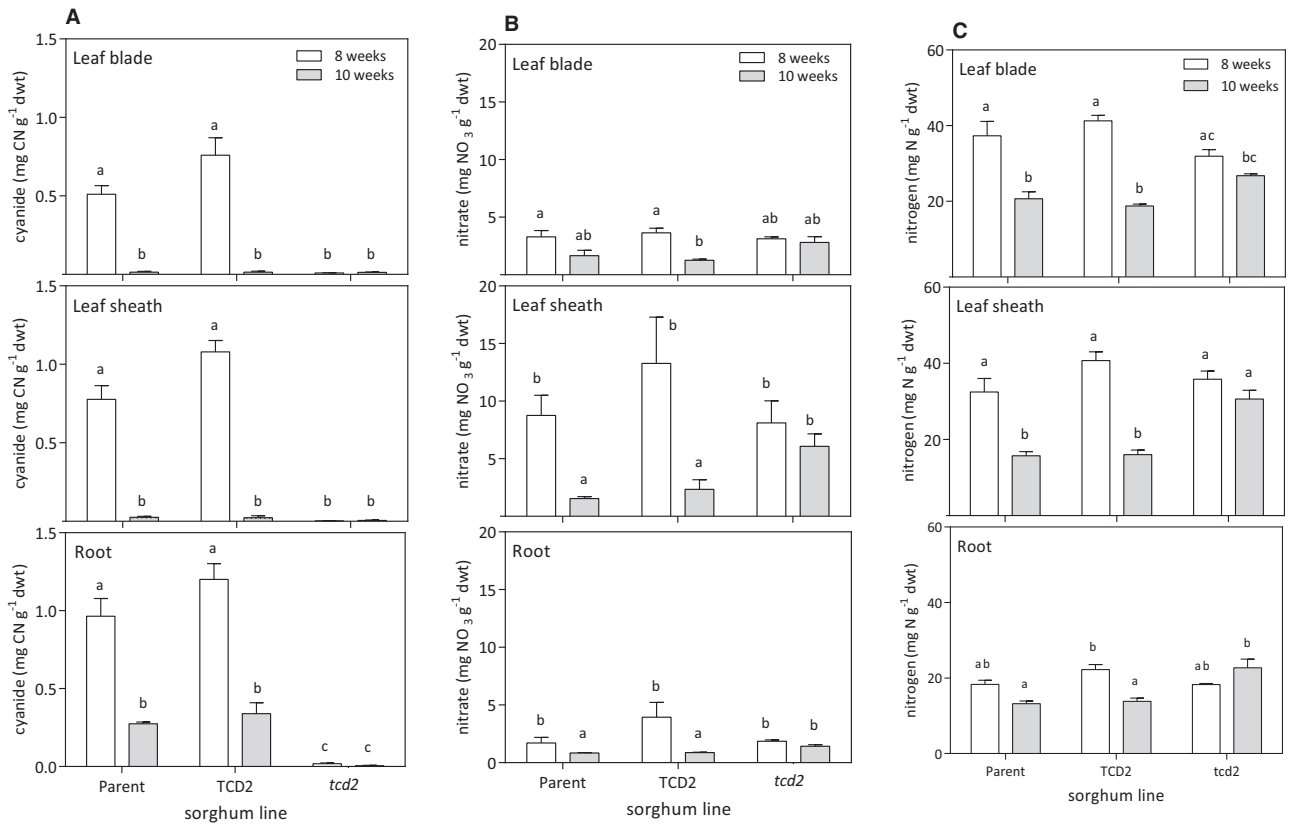

Fig. 3 (A) Hydrogen cyanide potential (mg g^{-1} DW); (B) nitrate (mg g^{-1} DW); and (C) nitrogen (mg g^{-1} DW) content of the leaf blade, leaf sheath and roots of parental control, *TCD2* and *tcd2* sorghum lines at 8 and 10 weeks post-germination. Values are the mean (±1 SE) data for $n = 4$ plants. Letters indicate a significant difference at $P < 0.05$, using Tukey's tests.

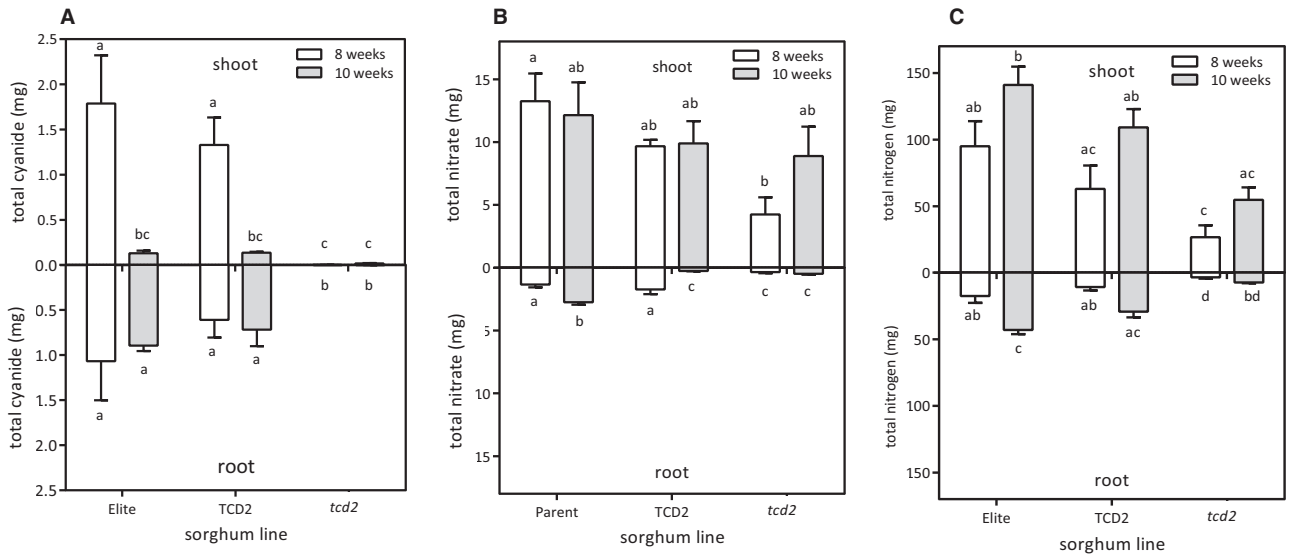

Fig. 4 (A) Total hydrogen cyanide potential, (B) total nitrate and (C) total nitrogen content in the shoots and roots of plants harvested 8 and 10 weeks after germination. Values are the mean (± 1 SE) data for $n = 4$ plants. Letters indicate a significant difference at $P < 0.05$, using Tukey's tests.

tcd2 plants reflect the same trends as the shoots, but with a quarter of the nitrogen content (**Fig. 4C**).

Nitrogen allocation

The proportion of nitrogen allocated to dhurrin formation (represented by CN^--N/N%; **Fig. 5A**) and the proportion of nitrogen allocated to nitrate (represented by NO_3^--N/N%; **Fig. 5B**) were calculated for the leaf blade, leaf sheath and roots for all plants from the two harvest time points. Overall, the proportion of nitrogen allocated to dhurrin formation in the parental and *TCD2* control plants was higher in the roots than in the shoots (**Fig. 5A**). The shoot and root CN^--N/N%

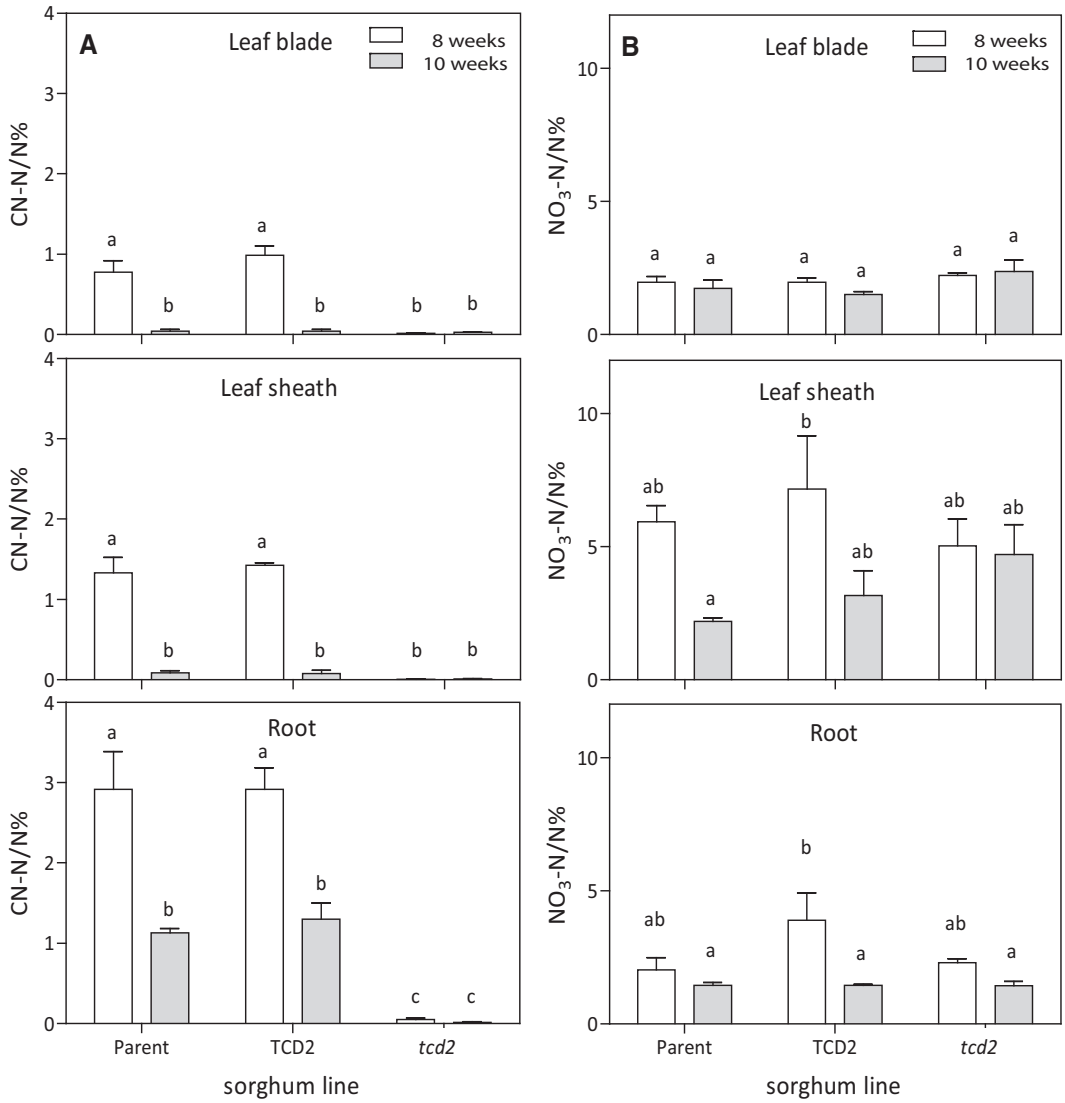

Fig. 5 Proportion of the total nitrogen pool present in (A) HCN (represented by CN^--N/N%) and (B) nitrate (represented by NO_3^--N/N%) in parental control, *TCD2* and *tcd2* sorghum plants at 8 and 10 weeks after germination. Values are the concentration of nitrogen present as cyanide (CN-N) or nitrate (NO_3-N) as a proportion of the concentration of total nitrogen (N). Values are the mean (± 1 SE) data from $n = 4$ plants. Tukey's post-hoc tests were performed, and letters indicate a significant difference at $P < 0.05$.

decreased with time. The proportion of nitrogen allocated to nitrate differed depending on the tissue type. In the leaf blade, NO_3^--N/N% was not significantly different between plant lines at the two harvest time points 1 ($P = 0.516$) and 2 ($P = 0.239$; **Fig. 5B**). In the leaf sheath, there appeared to be a decrease in the NO_3^--N/N% allocation over time for the parent and *TCD2* plants, while the NO_3^--N/N% remained high in the *tcd2* line (**Fig. 5B**), but this difference was not significant (8-week-old plants, $P = 0.494$; 10-week-old plants, $P = 0.143$). There was no significant difference in the proportion of nitrogen allocated to nitrate in the roots of the three lines harvested 8 and 10 weeks post-germination ($P = 0.117$ and $P = 0.995$, respectively).

Liquid chromatography–mass spectrometry (LC-MS) analysis

Leaf tissue metabolites, extracted in MeOH, were analysed by LC-MS, and the resulting metabolite profiles of the parental and *TCD2* control plants and the *tcd2* mutant showed distinct pattern differences (**Fig. 6**). The proposed and confirmed identification of the compounds present is shown in **Table 1**, and the structures of the subset of metabolites identified in the *tcd2* plants are shown in **Fig. 1**. The parental and *TCD2* control plants displayed a major component eluting at 5.6 min, representing dhurrin (m/z 334, $[M+Na]^+$), which was absent from the *tcd2* plants (**Fig. 6**). Likewise, the three dhurrin glucosides identified by Pičmanová et al. (2015) in the sorghum BTx cultivar were present in the control plants (compounds 15–17), but absent from the *tcd2* mutant. The 8-week-old parental control plants lacked two compounds assigned as caffeoylated dhurrin in the BTx line (Pičmanová et al. 2015), but they were present in the 2 week older control plants (8.6 and 8.9 min, data not shown) and absent from the *tcd2* mutant. The *tcd2* mutant line, on the other hand, contained a number of constituents previously identified as detoxification products derived from

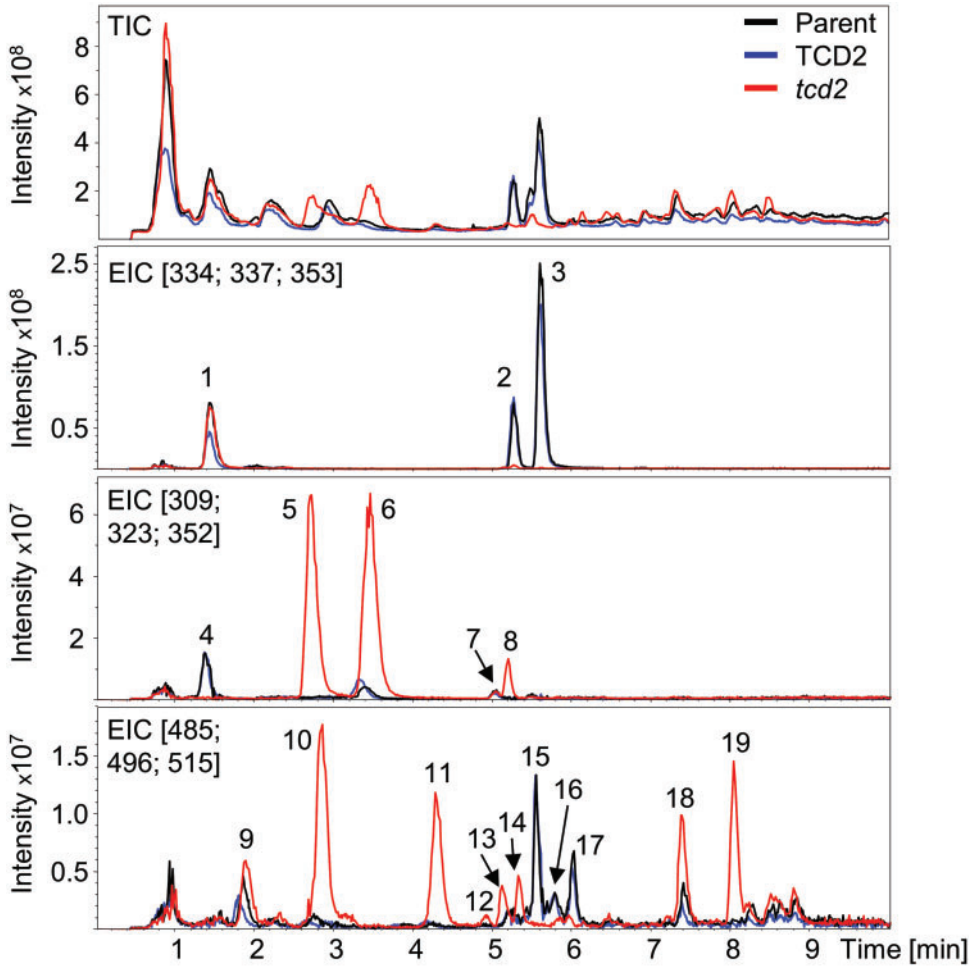

Fig. 6 Metabolite profiling of leaf tissue from 8-week-old parent (black), *TCD2* (blue) and *tcd2* (red) plants analyzed by LC-MS. TIC, total ion chromatograms; EIC, extracted ion chromatograms of relevant *m/z* values. Note the different scales on the *y*-axes. Compound assignments are shown in **Table 1**.

the biosynthetic intermediates of the dhurrin pathway in the Arabidopsis 2x plants expressing only *CYP79A1* and *CYP71E1* but not *UGT85B1* (Kristensen et al. 2005) (**Fig. 1**). More specifically, the *tcd2* line contained relatively high amounts of *p*-glucosyloxyphenylmethanol (2.7 min, *m/z* 309) (5), *p*-glucosyloxybenzoylglucose (2.9 min, *m/z* 485) (10) and *p*-glucosyloxybenzoic acid (3.5 min, *m/z* 323) (6). Interestingly, the latter was also found in the parental and *TCD2* control plants, although in smaller concentrations. In Arabidopsis these are all derived from *p*-hydroxybenzaldehyde, which is released concomitantly with HCN from the unstable cyanohydrin *p*-hydroxymandelonitrile, the product of CYP71E1 (Bak et al. 2000, Kristensen et al. 2005). The *tcd2* mutant plants also contained five additional compounds at *m/z* 485 with different retention times (11–14 and 19). These compounds were not detected in the non-mutated parent, *TCD2* sibling plants or the Arabidopsis 2x transgenic plants. At least four of these compounds may be assigned as either diglucosides or glucose-caffeic acid (CA) esters as supported by the presence of a major fragment ion for these compounds at *m/z* 347, corresponding to $[Glc\text{-}Glc\text{-}H_2O+Na]^+$ or $[Glc\text{-}CA\text{-}H_2O+Na]^+$ (Pičmanová et al. 2015). The glucosylated aglycon is likely to be *p*-hydroxybenzoic acid as in peak 6 and 7, *m/z* 323, and indeed compound 11 displays *m/z* 323 as a fragment ion, as does *p*-glucosyloxybenzoylglucose. Compound 13 displays the fragment *m/z* 185, corresponding to $[Glc\text{-}H_2O+Na]^+$, demonstrating that this compound is a diglucoside rather than a caffeoylated glucoside. Knowing that dhurrin glucosides and prunasin glucosides (Neilson et al. 2011) elute closely together and caffeoylated dhurrin significantly later, the closely eluting compounds 11–14 are suggested to be diglucosides and compound 19 a caffeoylated glucoside. The remainder of the suggested structures for the compounds listed in **Table 1** and **Fig. 1** are based on the fact that in the applied analytical system glucosides containing a free carboxylic acid group display molecular ions as both $[M+Na]^+$ and $[M+2Na\text{-}H]^+$, as seen for the known compounds 1, 2, 6 and 18 (**Table 1**). Arabidopsis 2x plants contain two more detoxification products, giving rise to signals at *m/z* 323, one likewise derived from *p*-hydroxybenzaldehyde (*p*-hydroxybenzoylglucose, compound 7) and another derived from the CYP79A1 product, *p*-hydroxyphenylacetaldoxime (*p*-glucosyloxyphenylethanol; **Fig. 1**).

Table 1 Dhurrin pathway-related metabolites identified by LC-MS analysis

Peak no.	Compound	t_R (min)	M[a] (*m/z*)	Fragment(s) (*m/z*)
1	Dhurrin acid	1.5	353 (375)	185
2	*p*-Glucosyloxyphenylacetic acid	5.3	337 (359)	185
3	Dhurrin	5.6	334	185; 307
4	Dhurrin amide	1.4	352	185
5	*p*-Glucosyloxyphenylmethanol[b]	2.7	309	185
6	*p*-Glucosyloxybenzoic acid	3.5	323 (345)	185
7	*p*-Hydroxybenzoyl glucose[c]	5.0	323	n.d.
8	Unidentified	5.2	309	185
9	Dhurrin acid glucoside[c]	1.9	515 (537)	347
10	*p*-Glucosyloxybenzoyl glucose[b]	2.9	485	185; 323
11	6-Glucoside[c,d]	4.3	485 (507)	323; 347
12	7-glucoside[c,d]	4.9	485	ND
13	7-Glucoside[c,d]	5.1	485	185; 347
14	6-Glucoside[c,d]	5.3	485 (507)	347
15	Dhurrin glucoside	5.6	496	ND
16	Dhurrin glucoside	5.8	496	ND
17	Dhurrin glucoside	6.0	496	ND
18	Caffeoyl-dhurrin acid	7.4	515 (537)	347
19	Caffeoyl-6[c,d]	8.0	485 (507)	347

Compound numbers refer to chromatograms in **Fig. 6**, and the chemical structures are shown in **Fig. 1**.
[a] *m/z* values: molecular ions detected as either $[M+Na]^+$ or $([M+2Na-H]^+)$.
[b] Compounds detected in the *tcd2* mutant and transgenic Arabidopsis 2x plants, but not in sorghum control plants.
[c] Suggested compound identities based on retention times, molecular ion *m/z* values, fragment data and co-occurrence with other compounds as explained in the text. The remainder of the compounds were identified by a combination of molecular ion *m/z* values, fragments and a direct comparison either with extracts of Arabidopsis 2x (Kristensen et al. 2005) or with t_R values from Pičmanová et al. (2015) who used the same analytical method. In the table, only key fragments relevant for identification are mentioned.
[d] Compounds detected only in the *tcd2* mutant.

One of these constituents was also present in low amounts in the *tcd2* and parental control plants, but it could not be definitively determined which one of the two. However, *p*-hydroxybenzoylglucose (compound 7) is the most likely candidate as this and compound 6 are presumably precursors of the previously mentioned *p*-glucosyloxybenzoylglucose (10) found in high amounts in the *tcd2* mutant. Another major constituent present in the sorghum parental control line was *p*-glucosyloxyphenylacetic acid (2), which has been suggested to be a product of an endogenous pathway for dhurrin turnover (Jenrich et al. 2007, Pičmanová et al. 2015). Interestingly, this compound was also present in the *tcd2* plants, although in much lower concentrations. In the *tcd2* plants this compound may be a detoxification product derived from *p*-hydoxyphenylacetaldoxime, although it is not found in the Arabidopsis 2x plants. The presence of this detoxification product in the *tcd2* sorghum plants, but not in Arabidopsis 2x, may reflect a difference in the detoxification response to perturbation of an endogenous pathway in sorghum compared with an introduced pathway in Arabidopsis.

Three compounds, in addition to those listed above, were identified in the sorghum BTx cultivar, namely dhurrin amide (4) and dhurrin acid (1) proposed to be formed by conversion of the nitrile functional group of the dhurrin molecule into amide and carboxylic acid functional groups, respectively, and caffeoyl-dhurrin acid (18). In the *tcd2* line, compounds 1 and 18 were present in concentrations comparable with parental and *TCD2* control plants, but the dhurrin amide was only detected in the control plants. A new compound with the same *m/z* value as caffeoyl-dhurrin acid could be detected in all plants (9), and, based on retention time and molecular ion and fragment data, this is suggested to be dhurrin acid glucose (e.g. a diglucoside).

Discussion

An ethyl methanesulfonate (EMS) mutagenesis and TILLING program resulted in the identification of a number of sorghum mutant lines with alterations in cyanogenic capacity. We have previously characterized *tcd* type 1 mutants with mutations in *CYP79A1*, which encodes the first committed step in dhurrin synthesis in sorghum (Blomstedt et al. 2012). Other acyanogenic variants were identified with disruptions in the *UGT85B1* gene which encodes a UDPG-dependent family 1 glycosyltransferase (Blomstedt et al. 2012). In contrast to *CYP79A1* mutants, which were phenotypically close to normal (Blomstedt et al. 2012), many of the *UGT85B1* mutant plants were stunted, with such poor seed set that they could not be easily maintained. The *tcd2* line characterized in the experiments reported here also grows poorly, but plants exhibited self-fertility and produced a small number of seeds. This line was thus maintained and offspring were characterized.

Sorghum plants homozygous for the Q149* premature stop codon mutation in UGTB81 (*tcd2*) are devoid of dhurrin. Morphological and chemical analyses of the plants were carried out at two harvest time points, as it is known that there are spatial and temporal changes in dhurrin, nitrates and total nitrogen during sorghum development (Miller et al. 2014). Key growth parameters determined at the two different harvest time points (8- and 10-week-old plants) showed that the *tcd2* plants display a stunted phenotype, with poor root growth and an altered nitrogen content compared with the control plants. This is particularly evident 10 weeks post-germination, where the *tcd2* plants show decreased growth, with a significantly reduced root : shoot ratio compared with parental control lines or *TCD2* siblings lacking the Q149* mutation. However, the *tcd2* plants contained the same Chl concentration and had similar F_v/F_m levels to the parental and *TCD2* control plants, indicating that their photosynthetic apparatus was not significantly impaired compared with the parental and *TCD2* control plants. It should be noted that the 10 weeks post-germination parental and *TCD2* control plants analyzed had booted, i.e. switched to a reproductive state (Vanderlip 1993), whereas the *tcd2* plants had not. The older leaves of the parental and *TCD2* control plants had begun to senesce whereas leaf I and III of the *tcd2* plants were still photosynthetically active. This suggests that the developmental program in the *tcd2* mutant plants was substantially delayed. HCN released from the cyanohydrin formed and aldoximes released from the incomplete channeling of the pathway intermediates inhibit the mitochondrial electron transport chain. We propose that the delay in growth and development is a consequence of the extra resources required for metabolic detoxification of the HCN released and for transport and storage of intermediates produced as a result of the incomplete dhurrin biosynthesis pathway. Growth and development could also be affected by the inability of the *tcd2* mutant to balance the supply of reduced nitrogen via endogenous turnover of dhurrin (Pičmanová et al. 2015). Transgenic Arabidopsis 2x plants expressing *CYP79A1* and *CYP71E1*, but not *UGT85B1*, also exhibited poor growth and reduced seed set (Kristensen et al. 2005). In these transgenic plants, *CYP79A1* and *CYP71E1* were expressed using the strong *Cauliflower mosaic virus* 35S promoter (Kristensen et al. 2005). In contrast, in the *tcd2* mutant, which formed the basis for our current studies, the native *CYP79A1* and *CYP71E1* promoters were driving the expression. In both plant species, lack of UGT85B1 activity resulted in plants with a stunted growth phenotype.

The LC-MS analyses of the *tcd2* sorghum mutant demonstrated a number of interesting aspects of dhurrin biosynthesis and turnover. First, the presence of substantial amounts of detoxification products and the stunted growth phenotype of the *tcd2* mutants indicate that the sorghum plant does not have an 'emergency brake' (feedback mechanism) to inhibit the initial steps of dhurrin biosynthesis when the glucosyltransferase activity required to complete the synthesis of dhurrin is lacking. Previous studies have shown that expression of *CYP79A1* and *CYP71E1* in young sorghum plants is largely controlled at the transcriptional level (Busk and Møller 2002). Such an emergency brake would thus be expected to have resided in controlling elements in their native promoter sequences. In the absence of an efficient feedback mechanism, the labile cyanohydrin is continuously produced, causing self-toxicity and growth retardation. The clustering of the genes involved in biosynthesis of cyanogenic glucosides may have evolved to reduce the risk of such self-toxicity effectively by optimizing the channeling of the intermediates through the entire pathway, possibly by minimizing the chances of chromosomal rearrangements if individuals hybridize with other plants which are polymorphic with respect to synthesis of cyanogenic glucosides (Takos et al. 2011, Takos and Rook 2012). This may also explain why a single highly specific glycosyltransferase in sorghum mediates the interaction with CYP79A1 and CYP91E1 to produce dhurrin, despite our observation that the sorghum genome database with the UGT85B1 sequence shows that there are >200 genes encoding family 1 UGTs present in the sorghum genome. Several of these UGTs would be expected to be highly promiscuous detoxification enzymes able to glucosylate compounds not normally encountered in the plant (Jones et al. 1999, Thorsøe et al. 2005, Hansen et al. 2009). Likewise, generation and characterization of transgenic plants expressing *CYP79A1* and *CYP71E1* showed that no endogenous co-expressed UGTs in Arabidopsis, tobacco or in grapevine hairy root cultures were capable of glycosylating the cyanohydrin intermediate of the dhurrin pathway. This is in spite of the presence of UGTs able to glucosylate efficiently the toxic intermediates accumulating when an incomplete dhurrin pathway was expressed, as was also observed with the *tcd2* mutant line in the current study (Bak et al. 2000, Tattersall et al. 2001, Franks et al. 2006). The relative importance of the substrate specificity of UGT85B1, compared with the requirement for tight spatially and temporally controlled association of UGT85B1 with the metabolon to avoid disruption of the dhurrin pathway is yet to be determined.

Clustal alignments reveal that there are no other UGTs in sorghum with >50% amino acid sequence identity to UGT85B1. It is known that sequence identity measures are not a good predictor of function for UGTs. However, homology modeling of UGT85B1 against plant UGTs for which the crystal structure has been determined has identified a number of regions that are implicated in acceptor molecule recognition and binding (Thorsøe et al. 2005, Osmani et al. 2009). These modeling experiments have also suggested that Loop B, which is located in the N-terminal domain of the UGT involved in glycosylation of cyanohydrins in different plant species, is important for protein–protein interactions during metabolon formation (Franks et al. 2008, Osmani et al. 2009, Kannangara et al. 2011). Our results show that a tight interaction of the membrane-bound Cyt P450s with the UGT is important to avoid escape and dissociation of the cyanohydrin before glucosylation. In Arabidopsis 2x plants, significant amounts of side products were derived from the oxime intermediate (Kristensen et al. 2005), whereas in the *tcd2* mutant the majority of detoxification products known from Arabidopsis were derived from the cyanohydrin as shown in **Fig. 1**. This could reflect that the CYP79A1 : CYP71E1 ratio in the transgenic

Arabidopsis plants was out of balance or that the native lipid environment in the sorghum ER membrane facilitates a stronger interaction between the Cyt P450s. However, as pointed out, the sorghum-specific *p*-glucosyloxyphenylacetic acid may be derived from the oxime in the mutant, meaning that some of this first intermediate may likewise have escaped in sorghum.

In the present study we found that *tcd2* plants did not accumulate dhurrin glucosides and caffeoylated dhurrin. This provides evidence that these compounds are formed by glucosylation and caffeoylation of pre-formed dhurrin, respectively. On the other hand, it appears that the enzymes performing these glucosylations and caffeoylations are quite promiscuous, as demonstrated by the presence of diglucosides or caffeic acid esters of *p*-hydroxybenzoic acid (*m*/*z* 485 peaks present in sorghum *tcd2* but not Arabidopsis 2x) and a presumed dhurrin acid glucoside (*m*/*z* 515, compound 9).

Analysis of the HCNp, nitrate and nitrogen composition of the *tcd2*, *TCD2* and parent lines also showed that blocking dhurrin synthesis alters the nitrogen status of the *tcd2* mutant. In 10-week-old plants there was an increase in the nitrate concentration, particularly in the leaf sheath of *tcd2*. It is possible that this is due to the release and detoxification of cyanohydrin-derived HCN and detoxification of the oxime, which leads to production of free NH_4^+. This will decrease the nitrate reductase activity by feedback regulation and thus cause accumulation of any nitrate taken up through the roots in the *tcd2* plants. However, an alternative explanation may be the smaller *tcd2* plant size, as there was no significant difference in the total nitrate content of the *tcd2* plants compared with control plants. The small size of the *tcd2* mutant may also account for the finding that there is no significant difference in total nitrogen of any of the lines, despite the high nitrogen concentration of the *tcd2* mutant at the second harvest compared with the control plants. Nitrate fertilizer has been shown to increase dhurrin content in sorghum, possibly via increased transcription of the biosynthetic genes (Busk and Møller 2002, Hayes et al. 2015, Neilson et al. 2015).

Cyanogenic glucosides are suggested to serve as nitrogen storage compounds (Møller 2010b, Gleadow and Møller 2014, Pičmanová et al 2015) in addition to their role in plant defense. Sorghum is known to metabolize dhurrin continuously during growth (Adewusi 1990, Busk and Møller 2002), with the rate of catabolism exceeding that of biosynthesis as plants mature, leading to a decrease in total dhurrin content (Busk and Møller 2002, Miller et al. 2014). This was also demonstrated in the present study by the decrease in total dhurrin content in the shoots of 10-week-old compared with 8-week-old sorghum plants. The endogenous turnover of cyanogenic glucosides to recover nitrogen was originally suggested to proceed via β-glucosidase- and α-hydroxynitrilase-catalyzed release of HCN according to the classical bioactivation pathway. This would be followed by β-cyanoalanine synthase- and nitrilase-mediated production of ammonia and incorporation into amino acids according to the general plant pathway for detoxification of HCN concomitant with ethylene formation (reviewed by Bjarnholt and Møller 2008). This is supported by a recent genome-wide association study showing that dhurrin content is associated with single nucleotide polymorphisms in regions where the closest genes are the two dhurrinases (β-glucosidases) responsible for dhurrin bioactivation (Hayes et al. 2015). Alternatively, nitrogen recovery may proceed via pathways that avoid release of toxic HCN. Picmanova et al. (2015) proposed three turnover or 'recycling' pathways for cyanogenic glucosides that would allow tight control of the defense response of the plant as well as preventing self-intoxication due to the release of toxic HCN during nitrogen recovery. In sorghum, such pathways involve dhurrin amide and dhurrin acid or *p*-glucosyloxyphenylacetic acid as products and intermediates proposed to be produced by enzymes acting directly on dhurrin without preceding hydrolysis by dhurrinases (Jenrich et al. 2007, Pičmanová et al. 2015). The finding that *tcd2* plants contain only trace amounts of *p*-glucosyloxyphenylacetic acid compared with the higher amounts present in the parent and *TCD2* plants supports that this compound is indeed derived from dhurrin in the wild-type plant. The minute amounts of the compound detected in the mutant could, as mentioned above, be produced as a detoxification of the oxime intermediate. On the other hand, dhurrin acid and its derivatives were found in similar concentrations in the *tcd2* mutant and parent and *TCD2* plants, suggesting that these compounds are not derived from dhurrin as otherwise proposed by Pičmanová et al. (2015). A plausible explanation is that the production of these compounds from dhurrin in the parental control plants proceeds via the bioactivation pathway and formation of the cyanohydrin, which is the end-product of biosynthesis in the mutant plants. This is supported by the finding that parental and *TCD2* plants contain appreciable amounts of glucosylated *p*-hydroxybenzoic acid (**Fig. 1**), presumably a detoxification product of *p*-hydroxybenzaldehyde formed concomitantly with HCN release from the cyanohydrin. In conclusion, LC-MS analysis of the UGT mutant supports that the compounds previously suggested by Pičmanová et al. (2015) and Jenrich et al. (2007) to be turnover products of dhurrin are in fact so, and that more than one such turnover pathway may be operating in sorghum. However, the results also suggest that the earlier hypotheses that nitrogen recovery from cyanogenic glucosides takes place via release of HCN are at least partly true. More experiments are required to elucidate the exact nature of the different pathways, and the *tcd2* line, described here, as well as the *tcd1* line mutated in the first gene of the dhurrin biosynthetic pathway (Blomstedt et al. 2012), will be useful for such studies.

Materials and Methods

Plant material

Selected plant lines used in this study were the *tcd2* mutant, identified by TILLING (Blomstedt et al. 2012), and two control lines, the non-mutated parental line and the *TCD2* sibling line (a segregating population without the mutation from the original selection; Dahmani-Mardas et al. 2010). Parent, *TCD2* and *tcd2* plants ($n = 4$ plants per harvest) were grown in individual pots containing 1 : 2 perlite : seed raising mix (Exfoliator and Debco Pty Ltd., respectively), supplemented with a slow release fertilizer (Grow Coat 5 g per 12 liters of soil) under glasshouse conditions with a natural photoperiod from

September to December (approximately 14 h day/10 h night) and 26 ± 7°C day/20 ± 5°C night temperatures with relative humidity of 52 ± 14% and 59 ± 12%, respectively. Plants were harvested 8 weeks (harvest time point 1) or 10 weeks (harvest time point 2) after seed germination. These two time points were chosen to capture the HCNp in control plants before and after the developmentally controlled reduction in dhurrin (Miller et al 2014). Parameters measured at the time of harvest were: sheath height, sheath width, leaf number, leaf blade length, leaf blade width, total leaf surface area, and F_v/F_m as an estimate of the PSII photosynthetic efficiency. Leaf length, leaf width and F_v/F_m measurements were carried out using the youngest fully expanded leaf (leaf I) and a slightly older leaf (leaf III). The plants were divided into sections representing the leaf blade, leaf sheath and root tissues, dried at 50°C and weighed before determination of dhurrin, nitrate concentrations, total carbon–nitrogen levels and metabolite profiling. For comparison by LC-MS analysis Arabidopsis plants expressing *CYP79A1* and *CYP71E1* (2x plants) were grown as described (Kristensen et al. 2005), and *tcd2* and *TCD2* plants were grown for 2 weeks on soil in pots (greenhouse, 28°C), and the above-ground parts of the plants were harvested and immediately extracted as described below.

Determination of cyanide potential (HCNp)

Dhurrin concentration was measured in the leaf blade, leaf sheath and roots based on their HCNp as determined following addition of an excess amount of β-glucosidase (β-D-glucoside glucohydrolase, Sigma, EC 3.2.1.21) to ensure complete hydrolysis of dhurrin in the accurately weighed dried ground tissue sample. Evolved HCN was captured in an NaOH solution and measured as NaCN in a colorimetric assay (Gleadow et al. 2012b). Total HCN (mg) released and the corresponding dhurrin content in shoots and roots were calculated from the total mass of the tissue.

LC-MS analysis

Leaf blade and leaf sheath from 8- and 10-week-old plants (harvest time points 1 and 2, respectively) were weighed and homogenized in liquid N_2. Samples (100–200 mg, accurately weighed dried tissue) were boiled in 85% MeOH (500 µl, 3 min) and immediately cooled on ice. Rosette leaves of Arabidopsis 2x plants and 2-week-old freshly harvested *tcd2* and *TCD2* plants were extracted whole in the same manner. The homogenate was centrifuged (10 min, 3,000 × *g*) and aliquots (20 µl) were diluted with H_2O (40 µl) and filtered through a membrane by centrifugation. LC-MS analysis was carried out by injection of aliquots (0.1 and 2 µl) into an Agilent 1100 Series LC (Agilent Technologies) linked to a Bruker HCT-Ultra ion trap mass spectrometer (Bruker Daltonics) (Gleadow et al. 2012a).

Nitrate and total nitrogen analysis

The content of soluble nitrate in plant material was measured using ground dried tissue (15 mg) (Cataldo et al. 1975). The concentration of total elemental nitrogen was measured using ground dried plant material (5 mg) with an Elementar Vario Micro Cube, CHNS analyzer with acetanilide (Merck) as an internal standard.

Allocation of nitrogen to dhurrin and nitrate

To determine if the allocation of nitrogen to dhurrin (CN^--N/N%) or nitrate (NO_3^--N/N%) varies between the mutant line and the non-mutated parental line, the following calculations were made:

$$CN^- - N/N\% = [(CN^- (\text{mg g}^{-1}\text{ dwt}) \times 14/26)/\text{Total nitrogen (mg g}^{-1}) \times 100$$

$$NO_3^- - N/N\% = [(NO_3^- (\text{mg g}^{-1}\text{ dwt}) \times 14/62)/\text{Total nitrogen (mg g}^{-1}) \times 100$$

Identification and characterization of the mutation in UGT85B1

Genomic DNA was extracted from plant tissue using the MagAttract DNA extraction kit (Qiagen) and *UGT85B1*-specific primers (designed to the 5′- and 3′-untranslated regions) used to amplify and sequence the 1,595 bp full-length gene (For 5′-GGGGTCGGGGATATTGTATT-3′ and Rev 5′-CAGAACCA CTTATTGCAAACTC-3′). PCR conditions were: 95°C for 5 min, 95°C for 30 s, 54°C for 30 s, 72°C for 2.5 min for 35 cycles; 72°C for 10 min; 4°C hold. The resulting PCR product (~1.6 kbp) was gel purified (Promega Wiazard Kit) according to the manufacturer's instructions and sequenced using the Applied Biosystems PRISM BigDye Terminator Mix. A BlastP protein search was conducted using the Sorghum genome database at Phytozome 10.2 (http://phytozome.jgi.doe.gov/pz/portal.html#!search) and NCBI databases (http://www.ncbi.nlm.nih.gov/) (June 8, 2015).

Statistical analysis

Results were analyzed using GraphPad Prism 5 (GraphPad Software Inc.). Data sets were tested for normality and homogeneity of variances prior to analysis. Data that were not normally distributed were log transformed. Comparison of two treatment groups was performed using a Student's *t*-test. A one-way analysis of variance (ANOVA) was performed on groups of plants that had more than two treatment groups. Means that were significantly different were compared post-hoc using Tukey's *t*-tests. Different letters in the figures indicate means of significant difference. Mean values are followed by one standard error of the mean (± 1 SEM). Rose plots were created in Microsoft Excel after normalizing the data to the maximum value for each trait.

Supplementary data

Supplementary data are available at PCP online.

Funding

This work was supported by the Australian Research Council (ARC) [Linkage Grant LP0774941 to R.M.G., J.D.H. and B.L.M. with Pacific Seeds Pty. Ltd.]; the ARC [Discovery Grant DP130101049 to R.M.G. and B.L.M.]; the Center for Synthetic Biology 'bioSYNergy' [supported by the University of Copenhagen Excellence Program for Interdisciplinary Research (to B.L.M.)]; the VILLUM research center of excellence 'Plant Plasticity'; the European Research Council [Advanced Grant to B.L.M. (ERC-2012-ADG_20120314, Project No: 323034)]; the Carlsberg Foundation (to B.L.M.); the School of Biological Sciences, Monash University [a Dean's PhD Scholarship to N.O.].

Disclosures

The authors have no conflicts of interest to declare.

Acknowledgements

We thank Samantha Fromhold for technical assistance, and Peter Stuart, University of Queensland for advice on growth of forage sorghum.

References

Adewusi, S.R.A. (1990) Turnover of dhurrin in green sorghum seedlings. *Plant Physiol.* 94: 1219–1224.

Bak, S., Kahn, R.A., Nielsen, H.L., Møller, B.L. and Halkier, B.A. (1998) Cloning of three A-type cytochromes P450, CYP71E1, CYP98, and CYP99 from Sorghum bicolor (L.) Moench by a PCR approach and identification by expression in *Escherichia coli* of CYP71E1 as a

multifunctional cytochrome P450 in the biosynthesis of the cyanogenic glucoside dhurrin. *Plant Mol. Biol.* 36: 393–405.

Bak, S., Olsen, C., Petersen, B., Møller, B. and Halkier, B. (1999) Metabolic engineering of p-hydroxybenzylglucosinolate in Arabidopsis by expression of the cyanogenic CYP79A1 from Sorghum bicolor. *Plant J.* 20: 663–671.

Bak, S., Olsen, C.E., Halkier, B.A. and Møller, B.L. (2000) Transgenic tobacco and Arabidopsis plants expressing the two multifunctional sorghum cytochrome P450 enzymes, CYP79A1 and CYP71E1, are cyanogenic and accumulate metabolites derived from intermediates in dhurrin biosynthesis. *Plant Physiol.* 123: 1437–1448.

Bjarnholt, N. and Møller, B.L. (2008) Molecules of interest: hydroxynitrile glucosides. *Phytochemistry* 69: 1947–1961.

Blomstedt, C.K., Gleadow, R.M., O'Donnell, N., Naur, P., Jensen, K., Laursen, T., et al. (2012) A combined biochemical screen and TILLING approach identifies mutations in *Sorghum bicolor* L. Moench resulting in acyanogenic forage production. *Plant Biotechnol. J.* 10: 54–66.

Bowles, D. and Lim, E.-K. (2010) Glycosyltransferases of small molecules: their roles in plant biology. In Encyclopedia of Life Sciences. John Wiley &Sons, Chichester, UK.

Busk, P.K. and Møller, B.L. (2002) Dhurrin synthesis in sorghum is regulated at the transcriptional level and induced by nitrogen fertilization in older plants. *Plant Physiol.* 129: 1222–1231.

Cataldo, D.A., Maroon, M., Schrader, L.E. and Youngs, V.L. (1975) Rapid colorimetric determination of nitrate in plant tissue by nitration of salicylic acid. *Commun. Soil Sci. Plant Anal.* 6: 71–80.

Dahmani-Mardas, F., Troadec, C., Boualem, A., Leveque, S., Alsadon, A., Aldoss, A., et al. (2010) Engineering melon plants with improved fruit shelf life using the TILLING approach. *PLoS One* 5: e15776.

Franks, T., Powell, K., Choimes, S., Marsh, E., Iocco, P., Sinclair, B., et al. (2006) Consequences of transferring three sorghum genes for secondary metabolite (cyanogenic glucoside) biosynthesis to grapevine hairy roots. *Transgen. Res.* 15: 181–195.

Franks, T.K., Yadollahi, A., Wirthensohn, M.G., Guerin, J.R., Kaiser, B.N., Sedgley, M., et al. (2008) A seed coat cyanohydrin glucosyltransferase is associated with bitterness in almond (Prunus dulcis) kernels. *Funct. Plant Biol.* 35: 236–246.

Gleadow, R., Bjarnholt, N., Jørgensen, K., Fox, J. and Miller, R. (2012a) Detection, identification and quantitative measurement of cyanogenic glycosides. *In* Research Methods in Plant Science: Soil Allelochemicals. Edited by Narwal, S.S., Szajdak, L. and Sampietro, D.A. pp. 283–310. International Allelopathy Foundation, Studium Press, USA.

Gleadow, R.M., Møldrup, M.E., O'Donnell, N.H. and Stuart, P.N. (2012b) Drying and processing protocols affect the quantification of cyanogenic glucosides in forage sorghum. *J. Sci. Food Agric.* 92: 2234–2238.

Gleadow, R.M. and Møller, B.L. (2014) Cyanogenic glycosides: synthesis, physiology, and phenotypic plasticity. *Annu. Rev. Plant Biol.* 65: 155–185.

Hansen, E.H.R., Osmani, S.A., Kristensen, C., Møller, B.L. and Hansen, J. (2009) Substrate specificities of family 1 UGTs gained by domain swapping. *Phytochemistry* 70: 473–482.

Hansen, K.S., Kristensen, C., Tattersall, D.B., Jones, P.R., Olsen, C.E., Bak, S., et al. (2003) The in vitro substrate regiospecificity of recombinant UGT85B1, the cyanohydrin glucosyltransferase from *Sorghum bicolor*. *Phytochemistry* 64: 143–151.

Hayes, C.M., Burow, G.B., Brown, P.J., Thurber, C., Xin, Z. and Burke, J.J. (2015) Natural variation in synthesis and catabolism genes influences dhurrin content in sorghum. *Plant Genome* 8: doi: 10.3835/plantgenome2014.09.0048.

Jenrich, R., Trompetter, I., Bak, S., Olsen, C.E., Møller, B.L. and Piotrowski, M. (2007) Evolution of heteromeric NIT4 complexes in Poaceae with new functions in nitrile metabolism. *Proc. Natl. Acad. Ci. USA* 104: 18848–18853.

Jensen, K., Osmani, S.A., Hamann, N.T., Naur, P. and Møller, B.L. (2011) Homology modeling of the three membrane proteins of the dhurrin metabolon: catalytic sites, membrane surface association and protein–protein interactions. *Phytochemistry* 72: 2113–2123.

Jones, P.R., Møller, B.L. and Hoj, P.B. (1999) The UDP-glucose:*p*-hydroxymandelonitrile-*O*-glucosyltransferase that catalyzes the last step in synthesis of the cyanogenic glucoside dhurrin in Sorghum bicolor. Isolation, cloning, heterologous expression, and substrate specificity. *J. Biol. Chem.* 274: 35483–35491.

Jørgensen, K., Rasmussen, A.V., Morant, M., Nielsen, A.H., Bjarnholt, N., Zagrobelny, M., et al. (2005) Metabolon formation and metabolic channeling in the biosynthesis of plant natural products. *Curr. Opin. Plant Biol.* 8: 280–291.

Kahn, R., Fahrendorf, T., Halkier, B. and Møller, B. (1999) Substrate specificity of the cytochrome P450 enzymes CYP79A1 and CYP71E1 involved in the biosynthesis of the cyanogenic glucoside dhurrin in Sorghum bicolor (L.) Moench. *Arch. Biochem. Biophys.* 363: 9–18.

Kahn, R.A., Bak, S., Svendsen, I., Halkier, B.A. and Møller, B.L. (1997) Isolation and reconstitution of cytochrome P450ox and in vitro reconstitution of the entire biosynthetic pathway of the cyanogenic glucoside dhurrin from sorghum. *Plant Physiol.* 115: 1661–1670.

Kannangara, R., Motawia, M.S., Hansen, N.K.K., Paquette, S.M., Olsen, C.E., Møller, B.L., et al. (2011) Characterization and expression profile of two UDP-glucosyltransferases, UGT85K4 and UGT85K5, catalyzing the last step in cyanogenic glucoside biosynthesis in cassava. *Plant J.* 68: 287–301.

Kristensen, C., Morant, M., Olsen, C.E., Ekstrøm, C.T., Galbraith, D.W., Møller, B.L., et al. (2005) Metabolic engineering of dhurrin in transgenic Arabidopsis plants with marginal inadvertent effects on the metabolome and transcriptome. *Proc. Natl. Acad. Sci. USA* 102: 1779–1784.

Laursen, T., Møller, B.L. and Bassard, J.-E. (2015) Plasticity of specialized metabolism as mediated by dynamic metabolons. *Trends Plant Sci.* 20: 20–32

Miller, R.E., Gleadow, R.M. and Cavagnaro, T. (2014) Age versus stage: does ontogeny modify the effect of phosphorus and arbuscular mycorrhizas on above- and below-ground defence in forage sorghum? *Plant Cell Environ.* 37: 929–942.

Møller, B.L. (2010a) Dynamic metabolons. *Science* 330: 1328.

Møller, B.L. (2010b) Functional diversifications of cyanogenic glucosides. *Curr. Opin. Plant Biol.* 13: 337–346.

Møller, B.L. and Conn, E.E. (1980) The biosynthesis of cyanogenic glucosides in higher plants. Channeling of intermediates in dhurrin biosynthesis by a microsomal system from Sorghum bicolor (linn) Moench. *J. Biol. Chem.* 255: 3049–3056.

Morant, A.V., Jørgensen, K., Jørgensen, B., Dam, W., Olsen, C.E., Møller, B.L., et al. (2007) Lessons learned from metabolic engineering of cyanogenic glucosides. *Metabolomics* 3: 383–398.

Neilson, E.H., Edwards, A.M., Blomstedt, C.K., Berger, B., Møller, B.L. and Gleadow, R.M. (2015) Utilization of a high-throughput shoot imaging system to examine the dynamic phenotypic responses of a C4 cereal crop plant to nitrogen and water deficiency over time. *J. Exp. Bot.* 66: 1817–1832.

Neilson, E.H., Goodger, J.Q.D., Motawia, M.S., Bjarnholt, N., Frisch, T., Olsen, C.E., et al. (2011) Phenylalanine derived cyanogenic diglucosides from Eucalyptus camphora and their abundances in relation to ontogeny and tissue type. *Phytochemistry* 72: 2325–2334.

Nielsen, K.A., Tattersall, D.B., Jones, P.R. and Møller, B.L. (2008) Metabolon formation in dhurrin biosynthesis. *Phytochemistry* 69: 88–98.

Osmani, S.A., Bak, S. and Møller, B.L. (2009) Substrate specificity of plant UDP-dependent glycosyltransferases predicted from crystal structures and homology modeling *Phytochemistry* 70: 325–347.

Paquette, S., Møller, B.L. and Bak, S. (2003) On the origin of family 1 plant glycosyltransferases. *Phytochemistry* 62: 399–413.

Pičmanová, M., Neilson, E.H., Motawia, M.S., Olsen, C.E., Agerbirk, N., Gray, C.J., et al. (2015) A recycling pathway for cyanogenic glycosides evidenced by the comparative metabolic profiling in three cyanogenic plant species. *Biochem. J.* 469: 375–389.

Sibbesen, O., Koch, B., Halkier, B.A. and Møller, B.L. (1995) Cytochrome P-450 is a multifunctional heme-thiolate enzyme catalyzing the conversion of L-tyrosine to p-hydroxyphenylacetaldehyde oxime in the biosynthesis of the cyanogenic glucoside dhurrin in Sorghum bicolor (L.) Moench. *J. Biol. Chem.* 270: 3506–3511.

Takos, A., Lai, D., Mikkelsen, L., Abou Hachem, M., Shelton, D., Motawia, M.S., et al. (2010) Genetic screening identifies cyanogenesis-deficient mutants of Lotus japonicus and reveals enzymatic specificity in hydroxynitrile glucoside metabolism. *Plant Cell* 22: 1605–1619.

Takos, A.M., Knudsen, C., Lai, D., Kannangara, R., Mikkelsen, L., Motawia, M.S., et al. (2011) Genomic clustering of cyanogenic glucoside biosynthetic genes aids their identification in Lotus japonicus and suggests the repeated evolution of this chemical defence pathway. *Plant J.* 68: 273–286.

Takos, A.M. and Rook, F. (2012) Why biosynthetic genes for chemical defense compounds cluster. *Trends Plant Sci.* 17: 383–388.

Tattersall, D.B., Bak, S., Jones, P.R., Olsen, C.E., Nielsen, J.K., Hansen, M.L., et al. (2001) Resistance to an herbivore through engineered cyanogenic glucoside synthesis. *Science* 293: 1826–1828.

Thorsøe, K.S., Bak, S., Olsen, C.E., Imberty, A., Breton, C. and Møller, B.L. (2005) Determination of catalytic key amino acids and UDP sugar donor specificity of the cyanohydrin glycosyltransferase UGT85B1 from Sorghum bicolor. Molecular modeling substantiated by site-specific mutagenesis and biochemical analyses. *Plant Physiol.* 139: 664–673.

Till, B.J., Colbert, T., Tompa, R., Enns, L.C., Codomo, C.A., Johnson, J.E., et al. (2003) High-throughput TILLING for functional genomics. *Methods Mol. Biol.* 236: 205–220.

Vanderlip, R.L. (1993) How a Sorghum Plant Develops. Contribution No. 1203, Agronomy Department, Kansas Agricultural Experiment Station.